available at www.sciencedirect.com

SCIENCE DIRECT®

journal homepage: www.ejconline.com

TRF2 inhibition triggers apoptosis and reduces tumourigenicity of human melanoma cells ☆

Annamaria Biroccio[a,], Angela Rizzo[a], Raffaella Elli[b], Catherine-Elaine Koering[c], Aurélie Belleville[c], Barbara Benassi[a], Carlo Leonetti[a], Malcolm F.G. Stevens[d], Maurizio D'Incalci[e], Gabriella Zupi[a], Eric Gilson[c,f]*

[a]*Experimental Chemotherapy Laboratory, "Experimental Research Centre", Regina Elena Cancer Institute, Via delle Messi d'Oro 156, Rome 00158, Italy*
[b]*Cellular Biotechnology and Haematology Department, University "La Sapienza", Rome, Italy*
[c]*Laboratoire de Biologie Moléculaire de la Cellule de l'Ecole Normale Supérieure, CNRS UMR5161, IFR128, Lyon, France*
[d]*Center for Biomolecular Sciences, School of Pharmacy, The University of Nottingham, Nottingham, UK*
[e]*Department of Oncology, Pharmacological Research Institute "Mario Negri", Milan, Italy*
[f]*Service "Biologie des Tumeurs Solides – Génomique – Protéomique" Centre Hospitalier Lyon-Sud, France*

ARTICLE INFO

Article history:
Received 6 September 2005
Received in revised form
23 January 2006
Accepted 21 March 2006
Available online 5 June 2006

Keywords:
TRF2
G4-ligand
Anti-telomere therapy

ABSTRACT

The inhibition of the telomere-binding protein TRF2, by expressing the dominant negative form TRF2$^{\Delta B\Delta C}$, has been used as a model of anti-telomere strategy to induce a reversion of the malignant phenotype of M14 and JR5 human melanoma lines. Over-expression of TRF2$^{\Delta B\Delta C}$ induced apoptosis and reduced tumourigenicity exclusively in JR5 cells. p53 and Rb status and apoptotic response to DNA damage did not seem to account for the different response of the two lines to TRF2 inhibition. Interestingly, JR5 cells possess shorter and more dysfunctional telomeres compared to M14 line. Moreover, the treatment with the G-quadruplex-interacting agent (G4-ligand) RHPS4 sensitises M14 cells to TRF2 inhibition. These results demonstrate that TRF2 can impair tumourigenicity of human cancer cells. They further suggest that a basal level of telomere instability favours an efficient response to TRF2 inhibition and that a combined anti-TRF2 and G4-ligand therapy would have synergistic inhibitory effects on tumour cell growth.

1. Introduction

Telomere maintenance is important to all dividing cells, including cancer cells. Functional telomeres are essential for genomic stability and without mechanisms maintaining telomeres cells activate pathways leading to cell cycle arrest or apoptosis.[1] Activation of telomerase is crucial in telomere maintenance for most cancer cells.[2] In pre-clinical studies, some telomerase inhibitors have shown promise as effective agents for a wide variety of malignancies. However, with many, but not all telomerase therapeutic approaches, senescence or apoptosis has been observed only when the telomeres reach a critically short length.[3,4] Conversely, directly targeting telomeric structures might have immediate and profound effects on cell physiology. For instance, results from our group and others indicate that G4-ligands might disrupt

☆ Grant support: Supported by grants from "Associazione Italiana Ricerca sul Cancro" (A.I.R.C.), "Ministero della Salute", "CNR-MIUR", "La Ligue Nationale contre le Cancer" and "Canceropole program EPIMED". A. Rizzo is recipient of a fellowship from Italian Foundation for Cancer Research (F.I.R.C.).

* *Corresponding author:* Tel.: +39 6 52662569; fax: +39 6 52662592.
E-mail address: biroccio@ifo.it (A. Biroccio).

0959-8049/$ - see front matter © 2006 Elsevier Ltd. All rights reserved.
doi:10.1016/j.ejca.2006.03.010

telomere maintenance in cancer cells, making these compounds attractive anti-cancer agents.[5,6] Indeed, the very end of telomeric DNA corresponds to a G-rich 3′ overhang capable of forming G4 structures in physiological conditions, which might modulate several important telomere functions, including chromosome end protection and telomerase activity. The formation of these structures is certainly highly regulated in the cells[7] and might enter into competition with the folding of a t-loop, which appears to result from the invasion of the 3′ overhang into the duplex part of telomeric DNA.[8]

TRF2 is a ubiquitously expressed protein binding directly to the tandem array of duplex telomeric repeats and involved in telomere structure and chromosome end protection.[9–12] For example, inhibition of TRF2 induces end-to-end chromosome fusions and growth arrest or apoptosis.[11,13–15] TRF2 activates the rate of telomere degradation in the absence of telomerase possibly by promoting intra-molecular recombinations within telomeric repeats.[16–18] Interestingly, some of these TRF2 functions might result from its ability to modify the conformation of the telomeric DNA, for instance by promoting t-loop formation.[8] In addition to TRF2, many proteins involved in DNA damage response, particularly those involved in responding to double-strand breaks, also play key roles in telomere maintenance.[19] Understanding the mechanisms governing the cellular response to telomere dysfunction may facilitate the design of agents that selectively disrupt telomere integrity in tumour cells.

2. Materials and methods

2.1. Cells and culture conditions

M14 and JR5 human melanoma lines were obtained from the biopsy of patients at the Surgery Department of Regina Elena Cancer Institute (Roma, Italy). M14 and JR5 cells showed similar growth behaviour *in vitro* with a doubling time of about 24 h. Moreover, the lines were highly tumourigenic when injected in immunosuppressed mice. H460 human non-small lung carcinoma has been used as positive control of p53 and Rb status. The tumour lines were maintained as monolayer cultures in RPMI-1640 (Gibco-BRL, Gaithersburg, MD, USA) supplemented with 10% foetal calf serum, 2 mM L-glutamine and antibiotics at 37 °C in a 5% CO_2–95% air atmosphere.

2.2. Treatments

The pentacyclic acridine, 3,11-difluoro-6,8,13-trimethyl-8*H*-quino[4,3,2-*kl*]acridinium methosulfate (RHPS4) was synthesised in Malcolm Stevens's lab. RHPS4 stock solution was prepared in PBS. The drug was added to the cells 24 h after plating. Clinical grade cisplatin (CDDP, Pronto Platamine) and adriamycin (ADR, Adriblastina) were obtained from Pharmacia (Milano, Italy). Drug dilutions were freshly prepared before each experiment.

2.3. Viral infection

Cells were infected overnight with amphotropic virus encoding either hTERT or the telomere-binding protein TRF2, or the dominant negative form of the gene, $TRF2^{\Delta B\Delta C}$. Viruses were generated as previously described.[20] Briefly, the Phoenix amphotropic packaging line was transfected with the following retroviral plasmids: pBabe (empty vector, encoding the gene for the puromycin resistance only), pBabe-hTERT, pBabe-Myc-TRF2, pBabe-Myc-$TRF2^{\Delta B\Delta C}$ (lacking the N and C terminal domains). Transfected cells were incubated for 48 h at 37 °C for virus production and the virus-containing medium was collected, filtered (0.45 μm filter) to remove packaging cells and used to infect the target cells.

2.4. Proliferation assay

5×10^4 cells were seeded in 60-mm Petri plates (Nunc, Mascia Brunelli, Milano, Italy). Cell counts (Coulter Counter model ZM, Kontron) and viability (trypan blue dye exclusion) were determined daily, from day 1 to day 9 of culture.

2.5. Evaluation of apoptosis

Apoptosis was detected by flow cytometric analysis of annexin V staining. Annexin V–FITC *versus* PI assay (Vibrant apoptosis assay, V-13242, Molecular Probes, Eugene, OR, USA) was performed as previously described.[21] Briefly, adherent cells were harvested and suspended in the annexin-binding buffer (1×10^6 cells/ml). Thereafter, cells were incubated with annexin V–FITC and PI for 15 min at room temperature in the dark and immediately analysed by flow-cytometry. The data are presented as bi-parametric dot plots showing annexin V–FITC green fluorescence versus PI red fluorescence.

2.6. Western blotting

Western blot was performed as previously reported.[20] Forty micrograms of total proteins were loaded from each sample on denaturing SDS–PAGE. Detection of TRF2, p53 and Rb was done using anti-TRF2 mAb (4A794, Imgenex, San Diego, CA, USA; 1:1000), anti-p53 mAb (DO-1, Santa Cruz Biotechnology, Santa Cruz, CA, USA; 1:1000) and anti-Rb (G3-245 BD PharMigen, San Jose, CA, USA; 1:1000). ECL was used for detection. To check the amount of proteins transferred to nitrocellulose membrane, β-Actin was used as control and detected by an anti-human β-actin mAb (Santa Cruz, 1:500). The relative amounts of the transferred proteins were quantified by scanning the auto-radiographic films with a gel densitometer scanner (Bio-Rad, Milano, Italy) and normalised to the related β-actin amounts.

2.7. Southern blotting

TRF determination was performed as previously reported.[20] Briefly, 15 μg of DNA were digested with 40 U of *Hinf*1 and electrophoresed on 0.8% agarose gel. Then, DNA was denatured, neutralised, transferred to a nylon membrane (Hybond N, Amersham International, Buckinghamshire, UK) and cross-linked with ultraviolet light. The membrane was hybridized with 5′-end [γ-^{32}P]deoxyadenosine triphosphate-labeled telomeric oligonucleotide probe $(TTAGGG)_3$ at 42 °C for 2 h in a rapid hybridization buffer (QuikHyb Hybridization Solution, Stratagene, La Jolla, USA). After washing, the filters were autoradiographed (Hyperfilm-MP; Amersham)

with an intensifying screen at −80 °C for 24 h and the autoradiographs were scanned and the mean telomere length calculated.

2.8. Cytogenetic analysis

Chromosome aberrations were evaluated as previously reported.[22] To obtain chromosome preparations, cells in the log phase of growth were incubated with 0.1 μg/ml colcemid for 2 h and trypsinised, then incubated with hypotonic 0.075 M KCl for 10 min, fixed with methanol to acetic acid (3:1 v/v), dropped onto frosted microscope slides, and air-dried overnight. Chromosome aberrations were blindly evaluated by two independent observers in Giemsa-stained metaphases from two grown cultures for each line and each treatment. Analysis was performed at day 3 of treatment. For all the experiments, metaphase preparations of the different cells were performed simultaneously under the same conditions. The χ^2 test was used for statistical analysis.

2.9. Promoter activity

Cells were co-transfected with 0.25 μg of PEQ-176 (Promega Corporation) and 1 μg of pGL3basic-p21 or pGL3basic-MDM2 promoters (generous gifts from Dr. Bert Vogelstein, Baltimore, MD, USA, and Dr. M. Oren, Rehovot, Israel, respectively). Transfection experiments were carried out in serum-free OPTIMEM medium by lipofectamine reagent (Gibco-BRL). Transfected cells were then maintained in 10% FCS medium and harvested 48 h after the end of transfection. Luciferase activity was measured using a luciferase assay system kit (Promega Corporation), as specified by the manufacturer, and normalised to β-galactosidase expression.

2.10. Tumourigenicity

CD-1 male nude (nu/nu) mice, 6–8 weeks-old and weighting 22–24 g, were purchased from Charles River Laboratories (Calco, Italy). All procedures involving animals and their care were as previously described.[23] To assess tumourigenicity, different numbers of tumour cells (from 4×10^3 to 1×10^6/mouse) were injected i.m. Animals (ten for each group) were observed daily to establish tumour take, time of tumour appearance and tumour weight.[23]

2.11. Real-time PCR

Total RNA was extracted by using the RNAeasy kit (Qiagen Inc., Valencia, CA, USA). Reverse transcription of 0.5 μg of RNA was performed with First-Strand c-DNA Synthesis Using SuperScript II using either polyA primer or random hexamer (Invitrogen, CA, USA). The polymerase chain reaction (PCR) was carried out using intercalation of SYBR green following the manufacturer's protocol (FailSafe TM Real-Time PCR System, Epicentre). Equally amounts of cDNA, as determined by picogreen intercalation (Molecular Probes, Inc., Eugene, OR, USA), were used to quantify the expression of the genes of interest, as well as of three reference genes (Rpl19, PBGD, β-actin). The sequences of the gene-specific primers are given upon request. Reactions were performed in duplicate from two separate RNA preparations. Relative gene expression was determined as previously described.[24]

2.12. Statistical analysis

The results are presented as means ± SD. Significant changes were assessed using Student's t test for unpaired data, and P values <0.05 were considered significant.

3. Results

3.1. TRF2 inhibition induces apoptosis and reduces tumourigenicity in JR5 but not in M14 melanoma cells

The two human melanoma lines M14 and JR5 were infected with amphotropic virus encoding the full length and the dominant negative form of TRF2. Western blot analysis shows the appearance of a truncated form of TRF2 in TRF2$^{\Delta B\Delta C}$-infected cells and an increase of TRF2 protein expression of ~2-fold in TRF2-infected cells compared to control line (Fig. 1A). Overexpression of full length or dominant-negative TRF2 did not alter the *in vitro* growth behaviour of the M14 line (Fig. 1B). Similarly, the proliferation of TRF2 and TRF2$^{\Delta B\Delta C}$-overexpressing JR5 cells is similar to that of control during the exponential phase of growth. Interestingly, we noticed a reduction in the number of JR5 cells expressing TRF2$^{\Delta B\Delta C}$ during the days of growth, while control and TRF2-overexpressing cells were in the plateau phase (Fig. 1B). Cytofluorimetric analysis of the annexin V *versus* PI staining revealed that over-expression of TRF2$^{\Delta B\Delta C}$ induced apoptosis in JR5 but not in M14 cells (Fig. 1C). The percentage of apoptosis was about 32% in TRF2$^{\Delta B\Delta C}$-expressing cells, while less than 5% of annexin V$^+$/PI$^-$ cells was found in cells infected with control or TRF2 retroviruses.

To verify that the inability of M14 cells to activate the apoptotic program following TRF2$^{\Delta B\Delta C}$ over-expression was not due to a general lack of apoptotic response, apoptosis has been evaluated after treatment with CDDP and ADR, two different DNA-damage agents (Fig. 2). Cytofluorimetric analysis of the annexin V revealed that apoptosis was similarly induced in both lines following treatment with the drugs. The percentage of the annexin V$^+$/PI$^-$ cells was about 35% and 45% in M14 and JR5 cells exposed to CDDP and ADR, respectively.

M14 and JR5 cells infected with control or TRF2$^{\Delta B\Delta C}$ were injected in nude mice and their tumourigenicity evaluated (Table 1). No difference in tumourigenic ability was observed in TRF2$^{\Delta B\Delta C}$-infected M14 cells compared to control line. All the *in vivo* end-points evaluated were superimposable regardless of modulation of TRF2 protein. Over-expression of TRF2$^{\Delta B\Delta C}$ in JR5 cells determined a significant reduction of tumourigenicity. With an inoculum of 1×10^6 control-virus infected cells, tumours developed in all the animals (10/10), while only 80% of mice had tumours following injection of 1×10^6 TRF2$^{\Delta B\Delta C}$ cells. This nicely correlates with an increased median time of tumour appearance and a decrease in tumour weight. Moreover, by decreasing the number of injected cells, the reduction of tumour formation due to TRF2$^{\Delta B\Delta C}$ was more pronounced with only 30% of tumour formation when 5×10^5 TRF2$^{\Delta B\Delta C}$-expressing cells were injected ($P < 0.01$). Thus,

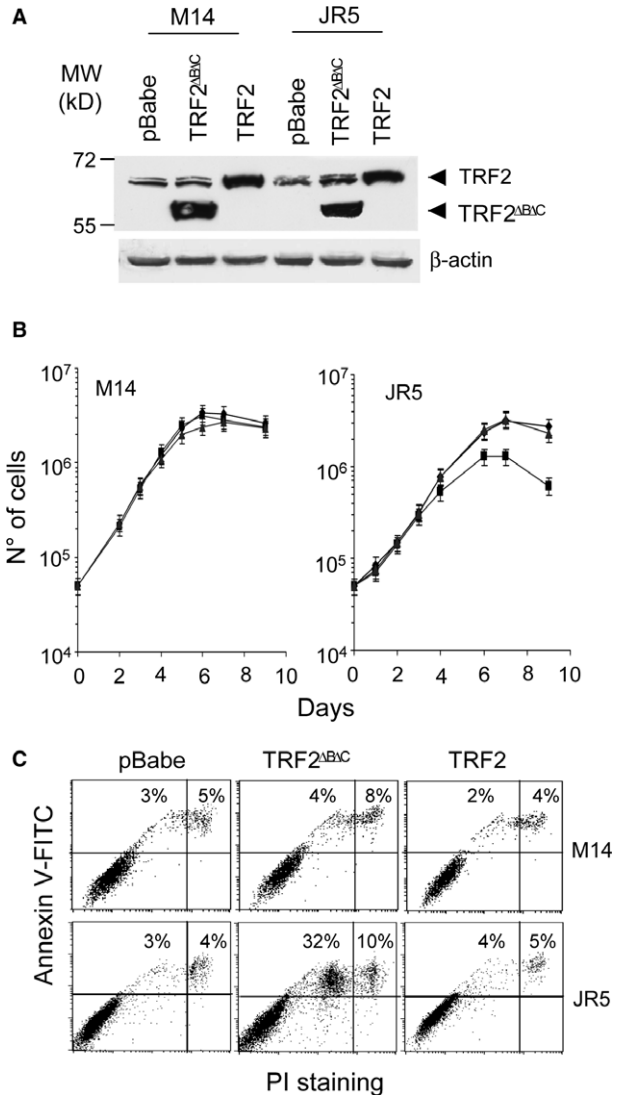

Fig. 1 – Over-expression of TRF2$^{\Delta B\Delta C}$ induces apoptosis in JR5 but not in M14 cells. (A) Western blot analysis of TRF2 protein expression in M14 and JR5 cells infected with control (pBabe), TRF2$^{\Delta B\Delta C}$ and TRF2 retroviruses. β-Actin protein expression was used as control of protein loading. (B) Proliferation assay of M14 and JR5 cells infected with control ♦, TRF2$^{\Delta B\Delta C}$ (■) and TRF2 retroviruses (▲). The figure shows representative experiments performed in quintuplicate with standard deviations (SD). (C) Bi-parametric dot plots showing annexin V *versus* PI staining in M14 and JR5 cells infected with control (pBabe), TRF2$^{\Delta B\Delta C}$ and TRF2 retroviruses. The percentages shown in the annexin V+/PI− and annexin V+/PI+ regions of each histogram represent the fraction of apoptotic and necrotic cells, respectively.

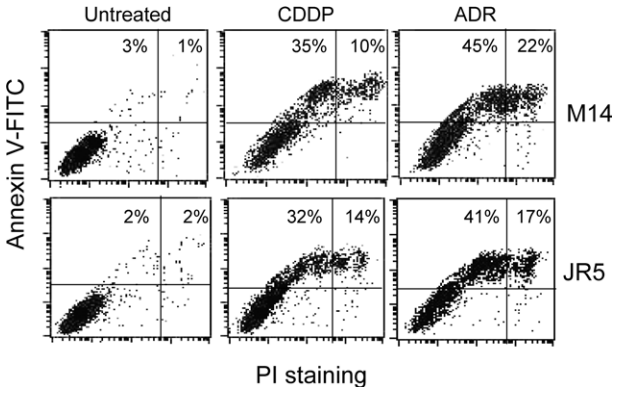

Fig. 2 – The inability of M14 cells to activate cell death following TRF2$^{\Delta B\Delta C}$ over-expression was not due to a lack of apoptotic response to DNA damage. Cytofluorimetric analysis of annexin V *versus* PI staining in M14 and JR5 cells treated with CDDP (12 μM for 12 h) and ADR (1 μM for 12 h). The percentages shown in the annexin V+/PI− and annexin V+/PI+ regions of each histogram represent the fraction of apoptotic and necrotic cells, respectively.

inhibition of TRF2 in JR5 cells is associated with an increase of apoptosis and a reduction of tumourigenic capacity *in vivo*.

3.2. *M14 and JR5 cells are p53 defective and Rb competent*

Because cells deficient for p53/Rb function failed to undergo apoptosis in response to TRF2$^{\Delta B\Delta C}$,[25] the status of p53 and Rb has been evaluated in M14 and JR5 cells. The sequencing analysis of the most mutated hot spots regions in the *p53* encoding sequence revealed that they were wild type in both lines (data not shown). Since a wild type sequence does not guarantee an intact p53 pathway, p53 protein expression and transcriptional activity were evaluated after genotoxic damage. No increase in p53 protein expression was observed both in M14 and JR5 cells treated with ADR (Fig. 3A). Consistent with these results, the activity of p21-LUC and MDM2-LUC was undetectable both in untreated and ADR-treated M14 and JR5 cells (Fig. 3B), while a marked increase in p53 protein expression and activity was evident in the H460 cells exposed to the DNA-damaging agent, chosen as control-positive line (Fig. 3A and B). Western blot analysis of Rb protein expression in proliferating and starved cells revealed that serum deprivation changed from hyper-phosphorylated to hypo-phosphorylated Rb protein in M14 and JR5 (Fig. 3C), indicating that both lines possess a functional Rb protein. Therefore, both melanoma lines are defective for p53 induction but functional for the cell cycle related functions of pRb. Thus, the different effect of TRF2$^{\Delta B\Delta C}$ in M14 and JR5 cells is unlikely to be explained by a differential functioning of the p53 or Rb pathways.

3.3. *JR5 cells display a higher level of telomere instability than M14 cells*

We next explored telomeres status of M14 and JR5 cells. As shown in Fig. 4A, telomere length of M14 cells ranged from 12 to 6 kb, with a mean length of ~9 kb, while it was significantly shorter in JR5 cells, ranging from 9 to 3 kb, with a mean of ~5 kb. This might result from the higher expression of *hTERT* and of its positive regulator *Tank1* mRNA (Table 2). The shorter telomeres in JR5 cells correlated with a decrease in end protection capacities. Indeed, compared to M14, JR5 cells had a higher number of telomeric fusions, harbouring a total of 40 *versus* 14 fusions out of 100 metaphases analysed ($p < 0.005$). The mean values of telomeric fusion frequency,

Table 1 – Tumourigenicity of control (pBabe) and TRF2$^{\Delta B\Delta C}$-infected M14 and JR5 cells

Lines	Number of cells/mouse	Number of tumours/ number of injections (%)	Median latency of tumour appearance in days (range)	Tumour weight (mg ± SD)
M14/pBabe	1×10^6	10/10 (100)	10 (10–14)	4690 ± 630
	5×10^5	10/10 (100)	24 (17–35)	2480 ± 340
	1×10^5	8/10 (80)	41 (38–59)	1310 ± 290
	2×10^4	6/10 (60)	65 (52–75)	660 ± 240
	4×10^3	2/10 (20)	NM	NM
M14/TRF2$^{\Delta B\Delta C}$	1×10^6	10/10 (100)	10 (10–17)	4220 ± 750
	5×10^5	10/10 (100)	22 (14–41)	2840 ± 510
	1×10^5	10/10 (100)	45 (35–47)	1570 ± 340
	2×10^4	6/10 (60)	59 (49–69)	580 ± 240
	4×10^3	2/10 (20)	NM	NM
JR5/pBabe	1×10^6	10/10 (100)	16 (16–26)	3200 ± 450
	5×10^5	10/10 (100)	47 (38–79)	1550 ± 320
	1×10^5	6/10 (60)	68 (54–80)	580 ± 125
	2×10^4	2/10 (20)	NM	NM
	4×10^3	0/10 (0)	NM	NM
JR5/TRF2$^{\Delta B\Delta C}$	1×10^6	8/10 (80)	72 (42–80)	390 ± 80
	5×10^5	3/10 (30)	NM	NM
	1×10^5	0/10 (0)	NM	NM
	2×10^4	0/10 (0)	NM	NM
	4×10^3	0/10 (0)	NM	NM

CD-1 male nude (nu/nu) mice, 6–8 weeks-old and weighting 22–24 g, were purchased from Charles River Laboratories (Calco, Italy). All procedures involving animals and their care were as previously described[23]. To assess tumourigenicity, different numbers of tumour cells (from 4×10^3 to 1×10^6/mouse) were injected i.m. Animals (10 for each group) were observed daily to establish tumour take, time of tumour appearance and tumour weight[23]. Tumour weight was calculated at day 80 after tumour cell injection. NM, not measurable.

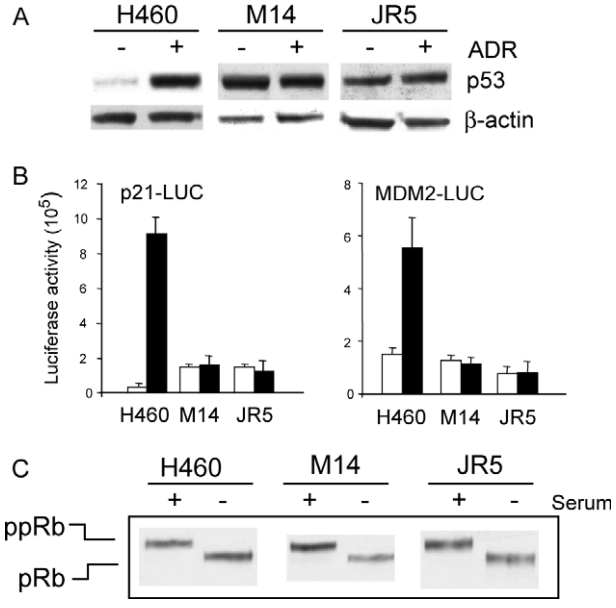

Fig. 3 – M14 and JR5 cells possess a non-functional p53 and an active Rb protein. (A) Western blot analysis of p53 protein expression in M14 and JR5 cells untreated (–) and treated (+) with ADR (1 μM for 24 h). (B) Activity of p21 and MDM-2 p53-responsive promoters in M14 and JR5 cells untreated (–) and treated with ADR (+). (C) Western blot analysis of Rb protein expression in proliferating (+) and serum-starved (–) M14 and JR5 cells. H460 human cancer cells were used as positive control for p53 and Rb assay. β-Actin protein expression was used as control of protein loading.

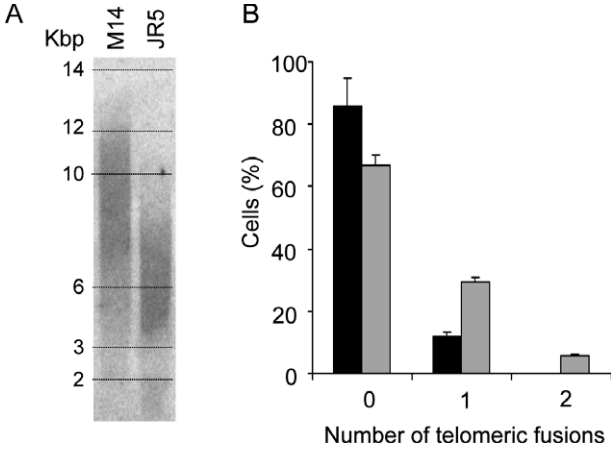

Fig. 4 – M14 cells possess a different telomere status compared to JR5 line. (A) Terminal restriction fragment measured by Southern blot in M14 and JR5 human melanoma cells hybridized with the telomeric repeat $(TTAGGG)_3$. A representative out of three independent experiments is shown. (B) Percentage of cells with 0, 1 and 2 telomeric fusions/total number of metaphases analysed in M14 (black columns) and JR5 (grey columns) cells. The data represent the mean of three independent experiments with standard deviation (SD).

Table 2 – Gene expression of multiple telomeric proteins in M14 and JR5 human melanoma lines

Category	Gene	M14 expression[a]	JR5 expression[a]	M14/JR5
Telomeric complex	hTERT	5.82	1.36	4.26
	hEST1a	1.87	2.81	0.66
	TRF1	18.62	22.66	0.82
	TRF2	4.79	2.02	2.37
	rap1	20.31	17.97	1.13
	tin2	4.64	6.44	0.72
	pinx1	1.10	1.81	0.61
	pot1	4.06	4.73	0.86
	est1b	8.92	14.70	0.61
Damage repair	tank2	6.43	9.40	0.68
	tank1	12.10	3.40	3.56
	blm	1.81	5.65	0.32
	WRN	3.42	0.94	3.63
	hMRE11A	0.36	0.13	2.83
	DNA PKC	113.68	70.78	1.61
	rad50	3.76	2.60	1.45
	ku70	74.09	61.82	1.20
	ku80	94.44	68.82	1.37
	nsb1	1.87	0.05	37.33
Damage response	ATM	28.18	57.47	0.49
	P16	0.62	0.62	1.00
	P21	1.41	0.28	5.07
	P53	130.62	94.90	1.38

Gene expression profile (by real-time PCR) of some telomeric protein complex and protein involved in damage–repair and response in M14 and JR5 cells. The PCR reactions were carried as reported in Section 2.
a Relative gene expression was determined as previously described.[24] The relative level of gene expression was calculated as a ratio of the quantity of interest gene and three reference genes (Rpl119, PBGD, β-actin).

calculated as number of end-to-end fusions/number of metaphases were 0.1 and 0.4 for M14 and JR5 cells, respectively (Fig. 4B).

mRNA expression by real-time PCR of a set of genes involved in telomere and DNA damage response (Table 2) revealed that the amount of *Pot1* mRNA appears similar in both lines suggesting that Pot1 dosage does not account for the differential capping and protection against TRF2 inhibition between the two lines.[26] Interestingly, the better capping in M14 than in JR5 correlates with a higher expression of the mRNA corresponding to the genes encoding the *Mre11–Rad50–Nbs1* (*MRN*) complex, in particular the *NBS1* gene.

3.4. *TRF2 inhibition sensitises M14 cells to telomere-damaging drug*

The correlation in JR5 cells between a high level of telomere instability and the sensitivity to $TRF2^{\Delta B\Delta C}$ expression suggests a synergistic effect between telomere uncapping and TRF2 inhibition. Therefore, we evaluated the response to the G4-ligand RHPS4, previously described as telomere-damaging agent,[5] in M14 cells with modulated TRF2 or hTERT. Fig. 5A shows the survival curves of control, hTERT, TRF2 and $TRF2^{\Delta B\Delta C}$-infected cells exposed to different concentration of RHPS4. Over-expression of either hTERT or TRF2 significantly decreased the cell toxicity of RHPS4, the survival of cells being about 40% in control cells and 80% in hTERT and TRF2-infected cells exposed to 1 μM RHPS4 concentration, respectively. Inhibition of TRF2, by expressing $TRF2^{\Delta B\Delta C}$, markedly reduced the survival of M14 cells treated with RHPS4 when compared to control and TRF2-infected cells (Fig. 5A). For instance, at 1 μM drug dose, the survival of $TRF2^{\Delta B\Delta C}$-expressing cells reached the value of about 15%. Cytofluorimetric analyses of annexin V *versus* PI staining show that the level of RHPS4 cytotoxicity correlated with apoptosis (Fig. 5B).

4. Discussion

The multiple roles of TRF2 in telomere structure and functions render it an interesting target for anti-telomere pharmacological interventions.

TRF2 inhibition, by expressing the dominant negative form $TRF2^{\Delta B\Delta C}$, has been used as a model of anti-telomere strategy to induce a reversion of the malignant phenotype of M14 and JR5, two telomerase-positive human melanoma lines. We found that over-expression of $TRF2^{\Delta B\Delta C}$ induced apoptosis and reduced tumourigenicity exclusively in JR5 cells. The inability of M14 line to respond to $TRF2^{\Delta B\Delta C}$ over-expression is not due to a lack of an apoptotic response to DNA damage because apoptosis is efficiently activated in M14 cells following treatment with the DNA-damaging agents cisplatin and adriamycin. Analysis of p53 and Rb status demonstrated that both melanoma lines are defective for p53 induction but functional for the cell cycle related functions of pRb. Thus, the different effect of $TRF2^{\Delta B\Delta C}$ in M14 and JR5 cells is unlikely to be explained by a differential functioning of the p53 or Rb pathways. Moreover, our data demonstrate that apoptosis induced

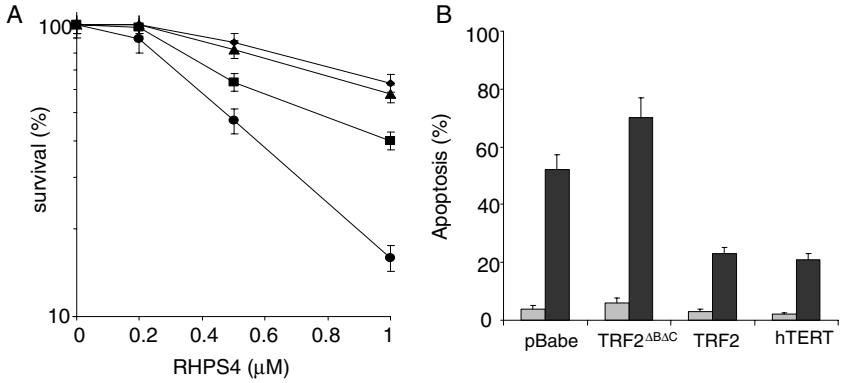

Fig. 5 – Increased telomere dysfunction renders M14 cells sensitive to TRF2 inhibition. (A) M14 cells infected with control (■), hTERT (♦), TRF2 (▲) and TRF2$^{\Delta B\Delta C}$ (●) retroviruses were exposed to different doses of the G4-ligand RHPS4, ranging from 0.2 to 1 μM. Surviving fractions were calculated as the ratio of absolute survival of the treated sample/absolute survival of the control sample. (B) Percentage of apoptotic cells calculated by annexin V assay in control (pBabe), hTERT, TRF2 and TRF2$^{\Delta B\Delta C}$-infected cells untreated (grey bars) and treated for five days with 0.5 μM RHPS4 (black bars). The data represent the mean of four independent experiments with standard deviations (SD).

by TRF2$^{\Delta B\Delta C}$ in JR5 cells is p53-independent. This result differs from a previously published work, which showed a p53 dependency of TRF2$^{\Delta B\Delta C}$-trigger apoptosis in several human and mouse cell lines[13] and is in agreement with a recent report demonstrating p53-independent apoptosis following TRF2$^{\Delta B\Delta C}$ expression in liver cells *in vivo*.[14] These discrepancies might be due to cell type difference in the response to DNA damage and telomere dysfunction.

We also found a correlation between the sensitivity to TRF2 inhibition and the capping capacities of the tumour cells. Analysis of telomere status demonstrated that JR5 cells have shorter telomeres compared to M14 cells. The shorter telomeres in JR5 cells correlate with a higher number of telomeric fusions, demonstrating that JR5 cells possess a basal degree of telomere dysfunction. Moreover, gene expression profile of multiple telomere-related proteins revealed that the better capping in M14 than in JR5 was associated with a higher expression of the mRNA corresponding to the genes encoding the *Mre11–Rad50–Nbs1* (MRN) complex, in particular the *NBS1* gene. This, together with the fact that TRF2 interacts with MRN,[27] suggests that the reinforced capping and TRF2-inhibition resistance of M14 cells relies on an increased level of the MRN complexes. Furthermore, we demonstrated that treatment with the G4-ligand RHPS4 sensitises M14 resistant cells to TRF2 inhibition through activation of apoptosis. On the contrary, over-expression of either hTERT or TRF2 renders cells resistant to the drug.

In conclusion, our results show that TRF2 inhibition can limit the proliferation of human cancer cells both *in vitro* and *in vivo*, thus strengthening TRF2 as an important target for the development of new anti-cancer therapies. The sensitivity to this inhibition depends, at least in part, upon the capping functions of the tumour cells. These findings suggest that the level of telomere instability in cancers can predict the efficacy of anti-TRF2 or anti-telomere therapeutics. Moreover, the combined action of both G4-ligand and anti-TRF2 molecules would represent an efficient strategy to eliminate tumour cells exhibiting a robust telomere capping. This work opens the way to test the response to telomere damage in a panel of tumour cell lines possessing different basal level of telomere dysfunction strengthening the use of TRF2-based molecular therapies.

Conflict of interest statement

None declared.

Acknowledgement

We thank Adele Petricca for her helpful assistance in typing the manuscript.

REFERENCES

1. de Lange T, Jacks T. For better or worse? Telomerase inhibition and cancer. *Cell* 1999;**98**:273–5.
2. Morin GB. The human telomere terminal transferase enzyme is a ribonucleoprotein that synthesizes TTAGGG repeats. *Cell* 1989;**59**:521–9.
3. Mergny JL, Riou JF, Mailliet P, Teulade-Fichou MP, Gilson E. Natural and pharmacological regulation of telomerase. *Nucleic Acids Res* 2002;**30**:839–65.
4. Biroccio A, Leonetti C. Telomerase as a new target for the treatment of hormone-refractory prostate cancer. *Endocr Relat Cancer* 2004;**11**:407–21.
5. Leonetti C, Amodei S, D'Angelo C, et al. Biological activity of the G-quadruplex ligand RHPS4 (3,11-difluoro-6,8,13-trimethyl-8 H-quino[4,3,2-kl]acridinium methosulfate) is associated with telomere capping alteration. *Mol Pharmacol* 2004;**66**:1138–46.
6. Duan W, Rangan A, Vankayalapati H, et al. Design and synthesis of fluoroquinophenoxazines that interact with human telomeric G-quadruplexes and their biological effects. *Mol Cancer Ther* 2001;**1**:103–20.
7. Zaug AJ, Podell ER, Cech TR. Human POT1 disrupts telomeric G-quadruplexes allowing telomerase extension in vitro. *Proc Natl Acad Sci USA* 2005;**102**:10864–9.
8. Griffith JD, Comeau L, Rosenfield S, et al. Mammalian telomeres end in a large duplex loop. *Cell* 1999;**97**:419–22.

9. Broccoli D, Smogorzewska A, Chong L, de Lange T. Human telomeres contain two distinct Myb-related proteins, TRF1 and TRF2. *Nat Genet* 1997;**17**:231–5.
10. Bilaud T, Brun C, Ancelin K, Koering CE, Laroche T, Gilson E. Telomeric localization of TRF2, a novel human telobox protein. *Nat Genet* 1997;**17**:236–9.
11. van Steensel B, Smogorzewska A, de Lange T. TRF2 protects human telomeres from end-to-end fusions. *Cell* 1998;**92**:401–13.
12. Ancelin K, Brun C, Gilson E. Role of the telomeric DNA-binding protein TRF2 in the stability of human chromosome ends. *BioEssay* 1998;**20**:879–83.
13. Karlseder J, Broccoli D, Dai Y, Hardy S, de Lange T. p53- and ATM-dependent apoptosis induced by telomeres lacking TRF2. *Science* 1999;**283**:1321–5.
14. Lechel A, Satyanarayana A, Ju Z, et al. The cellular level of telomere dysfunction determines induction of senescence or apoptosis in vivo. *EMBO Rep* 2005;**6**:275–81.
15. Celli GB, de Lange T. DNA processing is not required for ATM-mediated telomere damage response after TRF2 deletion. *Nat Cell Biol* 2005;**7**:712–8.
16. Ancelin K, Brunori M, Bauwens S, et al. Targeting assay to study the cis functions of human telomeric proteins: evidence for inhibition of telomerase by TRF1 and for activation of telomere degradation by TRF2. *Mol Cell Biol* 2002;**22**:3474–87.
17. Karlseder J, Smogorzewska A, de Lange T. Senescence induced by altered telomere state, not telomere loss. *Science* 2002;**295**:2446–9.
18. Wang RC, Smogorzewska A, de Lange T. Homologous recombination generates T-loop-sized deletions at human telomeres. *Cell* 2004;**119**:355–68.
19. d'Adda di Fagagna F, Teo SH, Jackson SP. Functional links between telomeres and proteins of the DNA-damage response. *Genes Dev* 2004;**18**:1781–99.
20. Biroccio A, Amodei S, Benassi B, et al. Reconstitution of hTERT restores tumorigenicity in melanoma-derived c-Myc low-expressing clones. *Oncogene* 2002;**21**:3011–9.
21. Biroccio A, Benassi B, Filomeni G, et al. Glutathione influences c-Myc-induced apoptosis in M14 human melanoma cells. *J Biol Chem* 2002;**27**:43763–70.
22. Biroccio A, Gabellini C, Amodei S, et al. Telomere dysfunction increases cisplatin and ecteinascidin-743 sensitivity of melanoma cells. *Mol Pharmcol* 2003;**63**:632–8.
23. Leonetti C, D'Agnano I, Lozupone F, et al. Antitumor effect of c-myc antisense phosphorothioate oligodeoxynucleotides on human melanoma cells in vitro and in mice. *J Natl Cancer Inst* 1996;**88**:419–29.
24. Livak KJ, Schmittgen TD. Analysis of relative gene expression data using real-time quantitative PCR and the 2(-Delta Delta CT). *Methods* 2001;**25**:402–8.
25. Chen X, Ko LJ, Jayaraman L, Prives C. p53 levels, functional domains, and DNA damage determine the extent of the apoptotic response of tumor cells. *Genes Dev* 1996;**10**:2438–51.
26. Yang Q, Zheng YL, Harris CC. POT1 and TRF2 cooperate to maintain telomeric integrity. *Mol Cell Biol* 2005;**25**: 1070–80.
27. Zhu XD, Kuster B, Mann M, Petrini JH, de Lange T. Cell-cycle-regulated association of RAD50/MRE11/NBS1 with TRF2 and human telomeres. *Nat Genet* 2000;**25**: 347–52.